PII: S0032-3861(97)00509-0

Polymer Vol. 39 No. 11, pp. 2299–2304, 1998

0032-3861/98/$19.00+0.00

Microstructure of thin films of photoluminescent semiconducting polymers

C. Y. Yang[a,b], Fumitomo Hide[b,c], María A. Díaz-García[b], Alan J. Heeger[b,c,d,*] and Y. Cao[e]
[a] *Materials Research Laboratory, University of California, Santa Barbara, CA 93106-5090, USA*
[b] *Institute for Polymers and Organic Solids, University of California, Santa Barbara, CA 93106-5090, USA*
[c] *Department of Physics, University of California, Santa Barbara, CA 93106, USA*
[d] *Department of Materials, University of California, Santa Barbara, CA 93106, USA*
[e] *UNIAX Corp., 6780 Cortona Drive, Santa Barbara, CA 93117, USA*
(Received 28 April 1997)

The polymer chain distribution in solution-cast thin films of poly(2-methoxy-5-(2′-ethylhexyloxy)-1,4-phenylene vinylene) (MEH-PPV) has been investigated by X-ray diffraction. The results show that regardless of the solvent, chain orientation in cast films is anisotropic; the PPV backbones and the planes defined by the benzene rings within the PPV backbones are predominantly parallel to the film plane. When drop-cast from tetrahydrofuran (THF), the preferred solvent for preparation of MEH-PPV films with low threshold in gain narrowing experiments, this anisotropy in chain orientation is more pronounced, and the crystallinity is higher. © 1998 Elsevier Science Ltd. All rights reserved.

(Keywords: X-ray diffraction; chain packing and crystal structure; MEH-PPV)

INTRODUCTION

The recent emergence of semiconducting π-conjugated polymers as solid-state laser materials was initiated by the demonstration of photopumped gain narrowing (collapse of the line width of the photoluminescent emission with increasing pump energy) by poly(2-methoxy-5-(2′-ethylhexyloxy)-1,4-phenylene vinylene) (MEH-PPV) with the aid of multiple scattering from titanium dioxide nanoparticles (to extend the path length in the gain medium)[1]. Photopumped gain narrowing was subsequently reported for neat, undiluted films of over a dozen conjugated polymers in planar waveguide structures[2–10]. Moreover, lasing has been observed in microcavity resonators from poly(1,4-phenylene vinylene) (PPV)[4] and a soluble PPV derivative, poly(2-butyl-5-(2′-ethyl-hexyl)-1,4-phenylene vinylene) (BuEH-PPV)[5], and from BuEH-PPV in distributed feedback structures[6].

For MEH-PPV, experiments have shown that the threshold for gain narrowing is highly dependent on the solvent from which the films were prepared[2,3]; films spin-cast from tetrahydrofuran (THF) showed lower pump energy thresholds for gain narrowing and narrower widths above threshold than other solvents, such as chlorobenzene (CB) or *p*-xylene. In this paper, we address the origin of the different behaviour of films cast from different solvents through studies of the chain orientation and microstructure.

The microstructure of a polymer film can be discussed at different levels: first, the molecular structure of the macromolecules; second, the chain packing and orientation of the macromolecules with respect to the substrate; and third, the degree of crystallinity and the size and orientation of the crystalline domains in the film. Since the macroscopic properties, such as the threshold for gain narrowing, are obtained from millimetre film areas and apparently depend on the microstructure, it is important to analyse the chain orientation and crystallinity in order to understand why films with the same molecular structure behave differently depending on the solvent from which they were cast.

We have investigated the microstructure of MEH-PPV of films cast from solution by X-ray diffraction. By relating the various structural features with the macroscopic properties of the films, we demonstrate a correlation between the microstructure and the utility of the polymer film for amplification of light by stimulated emission. X-ray diffraction scans from MEH-PPV films drop-cast from THF (the preferred solvent for gain narrowing performance) indicate a higher degree anisotropy of chain orientation with respect to the substrate, as well as higher crystallinity and larger crystalline domains, than films drop-cast from other solvents, such as CB or *p*-xylene.

EXPERIMENTAL

Free-standing MEH-PPV films were prepared in a nitrogen environment by drop-casting on glass substrates from different solvents (THF, *p*-xylene, or CB). Films were dried at room temperature for more than 24 h. Film thicknesses ranged between 5 and 10 μm.

Films of another alkoxy-substituted PPV derivative, poly(2-(3′,7′-dimethyloctyloxy)-5-methoxy-1,4-phenylene vinylene), DOM-PPV, were also prepared. The DOM-PPV served as a reference for analysis of the X-ray data from MEH-PPV films. The two polymers have a similar

---

* To whom correspondence should be addressed

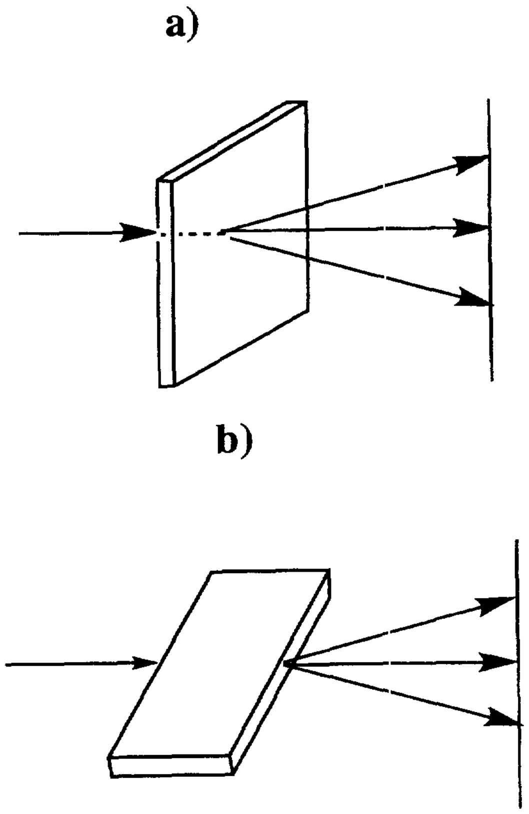

Figure 1 X-ray diffraction diagram: film perpendicular (a) and parallel (b) to the beam

molecular structure, but DOM-PPV is more crystalline. For specific measurements of crystal structure and packing, MEH-PPV and DOM-PPV films were stretched on a hot stage to a draw ratio of 5.

X-ray diffraction was performed primarily on a Siemens Smart-CCD diffractometer equipped with a rotation stage and a normal focus, 2.4 kW sealed tube X-ray source (Mo Kα radiation) operating at 50 kV and 40 mA. In addition, another X-ray diffractometer (Enraf–Nonius FR590), with Cu Kα radiation operating at 50 kV and 40 mA, was used for wide- and small-angle diffraction on stretched MEH-PPV and DOM-PPV films for structure determination. The films were set up primarily in two configurations, with the film plane perpendicular (perpendicular setting) and parallel (parallel setting) to the X-ray beam in the Siemens Smart-CCD diffractometer, as shown schematically in *Figure 1*. The diffraction data were processed on an IBM workstation with interactive data language (IDL).

RESULTS AND DISCUSSIONS

As noted above, a polymer film can be described as consisting of crystalline domains (crystallographic axes: $\boldsymbol{a}$, $\boldsymbol{b}$, $\boldsymbol{c}$) within amorphous regions. By convention, the polymer chain axis is designated as the $\boldsymbol{c}$-axis, the more direct chain packing direction as the $\boldsymbol{a}$-axis, and interchain direction which is related to the side chain length as the $\boldsymbol{b}$-axis. For the analysis of the microstructure of the film, we need to first know the crystal structure within the crystalline domains.

Crystal structure of MEH-PPV

The diffraction patterns of stretched MEH-PPV and DOM-PPV films, drop-cast from THF and aligned at a draw ratio of ~5, are illustrated in *Figure 2*. *Figure 2a* and *Figure 2b* are wide-angle diffraction patterns of MEH-PPV and DOM-PPV films respectively, whereas *Figure 2c* and *Figure 2d* are the small-angle diffraction patterns of the same films. Diffraction spots in *Figure 2b* are better separated than those in *Figure 2a* as a result of the better molecular ordering in DOM-PPV. These spots can be indexed as the 200 and 002 reflections, as indicated in *Figure 2a* and *Figure 2b*. In *Figure 2c* and *Figure 2d*, a diffraction spot is present along the equatorial direction, on each side of the centre beam (000 reflection), which can be indexed as 010. The distance from these 010 reflections to the central 000 reflection is shorter for the DOM-PPV sample, as expected, because of the longer side chains of DOM-PPV. Thus, the diffraction patterns of *Figure 2* show that the crystal structures of the two similar polymers are the same (although the $\boldsymbol{b}$-axis lattice parameters are different); the structures are orthorhombic with lattice parameters: $a = 0.712$ nm, $b = 1.605$ nm, and $c = 0.647$ nm for MEH-PPV; and $a = 0.712$ nm, $b = 2.089$ nm, $c = 0.647$ nm for DOM-PPV. The 0.356 nm d-spacing between the $\{200\}$ planes along the $\boldsymbol{a}$-axis is the distance between the planes defined by the benzene rings; the periodicity along the $\boldsymbol{b}$-axis being related to the length of the side chain, and the $\boldsymbol{c}$-axis to the chain axis, as described above. The unit cell consists of two monomer units; a projection view along the $\boldsymbol{a}$-axis is illustrated by the dashed lines in *Figure 3*. The crystal structures of MEH-PPV films drop-cast from p-xylene, CB, and THF are identical, as deduced from the X-ray diffraction data.

Anisotropic chain packing in MEH-PPV film

Figure 4a and *Figure 4b* show the diffraction patterns of an unstretched MEH-PPV film drop-cast from THF, with perpendicular and parallel settings respectively (see *Figure 1*). The diffraction pattern in *Figure 4a* shows a broad halo and a weak ring to the inside of it; the weak ring can be indexed as the 001 reflection. This means that the $\boldsymbol{c}$-axes (polymer chain axes) of the crystalline domains are isotropically distributed in the plane of the MEH-PPV film. On the other hand, in *Figure 4b*, strong arcs superposed on a weak broad halo are observed, showing a large anisotropy in the diffraction pattern. These arcs can be indexed as arising from 200 reflections that correspond to scattering from the $\{200\}$ planes defined by the benzene rings. These results indicate that the $\{200\}$ benzene ring planes within the crystalline domains are parallel to the plane of the film, with a correspondingly anisotropic distribution of the electron density (the diffraction intensity is governed by the electron density)[11,12]. This anisotropy is unique, i.e. the crystalline domains are aligned with the $\boldsymbol{c}$-axis and the benzene ring layers in the plane of the film, as shown schematically in *Figure 5*. This chain orientation anisotropy is consistent with that inferred from measurements of the refractive index[3].

The diffraction patterns for MEH-PPV films drop-cast from p-xylene and CB have similar features. However, there are clear differences in the degree of anisotropy of the chain packing, the crystallinity and the size of the crystalline domains. *Figure 6a–c* are the intensity profiles (normalized to the maximum peak intensity) of the diffraction patterns for MEH-PPV films drop-cast from THF, p-xylene and CB respectively. The profiles were obtained in two directions: parallel (continuous line) and perpendicular (dashed) to the [200] direction (*Figure 4b*).

The degree of anisotropy of the chain packing was

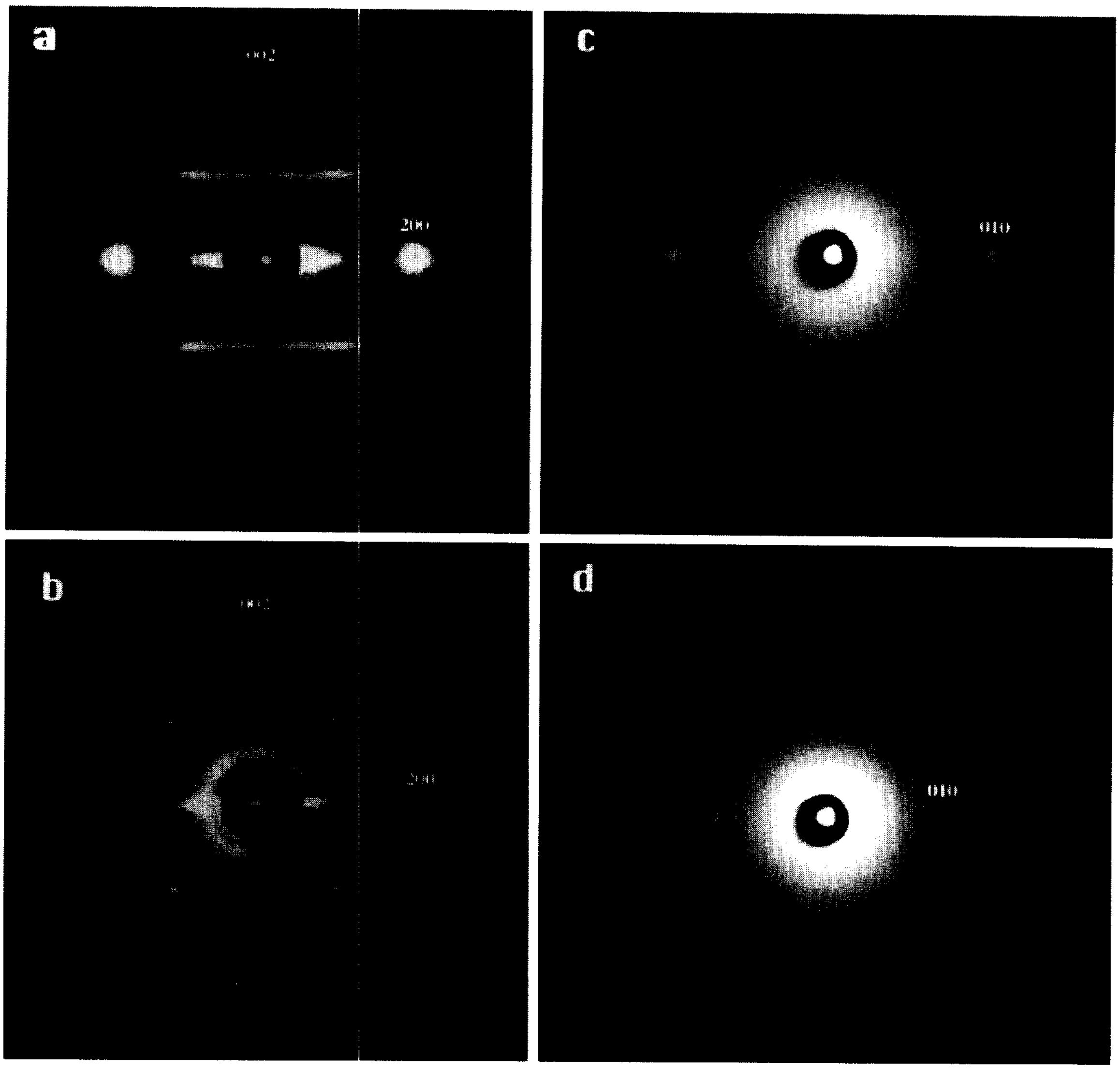

Figure 2 Diffraction patterns of stretched MEH-PPV and DOM-PPV films (drop-cast from THF). (a) MEH-PPV, wide-angle diffraction pattern; (b) DOM-PPV, wide angle; (c) MEH-PPV, small angle; and (d) DOM-PPV, small angle

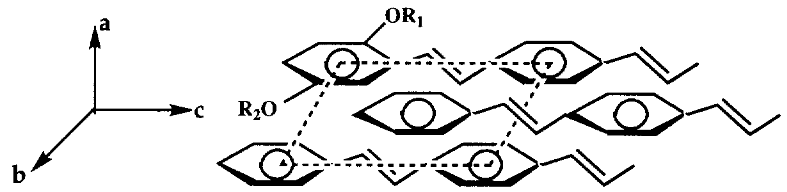

Figure 3 Schematic drawing of the projection of the unit cell of MEH-PPV along ***a***-axis. The side chains OR$_1$ and OR$_2$ were drawn only on one benzene ring for clarity. R$_1$ = CH$_3$, R$_2$ = CH[(CH$_2$)$_5$–CH$_3$)](CH$_3$)

estimated by measuring the intensity in two directions: along the [200] direction (continuous line in *Figure 6a–c*) and perpendicular to it (broken line in *Figure 6a–c*). From these data, we determined the ratio of the intensity of the 200 reflection in the [200] direction to the total intensity in the two directions. The ratios are approximately 80%, 60%, and 60% for MEH-PPV from THF, *p*-xylene and CB respectively, implying that the percentage of the benzene ring planes that are oriented in-plane for films cast from THF, xylene and CB are different. Therefore, the degree of the anisotropy of the films is somewhat different depending on the solvent.

The degree of crystallinity is estimated from the ratio of the integrated normalized scattering under the resolved crystalline peaks to the total scattered intensity; the ratios are approximately 40%, 20%, and 20% for films cast from THF, *p*-xylene and CB respectively[13]. From the widths of the diffraction peaks, we infer the coherence lengths of the ordered crystalline domains (as estimated by using Debye–Sherrer formula) to be approximately 7 nm for THF and 5 nm for both *p*-xylene and CB[11].

Thus, the results indicate that better performance as a gain narrowing material is correlated with a higher degree of in-plane chain (backbone) orientation, with higher crystallinity, and with longer structural coherence lengths. The in-plane chain orientation might be the essential factor for gain narrowing, i.e. the essential factor is the anisotropy in the oscillator strength of the π–π^* absorption which

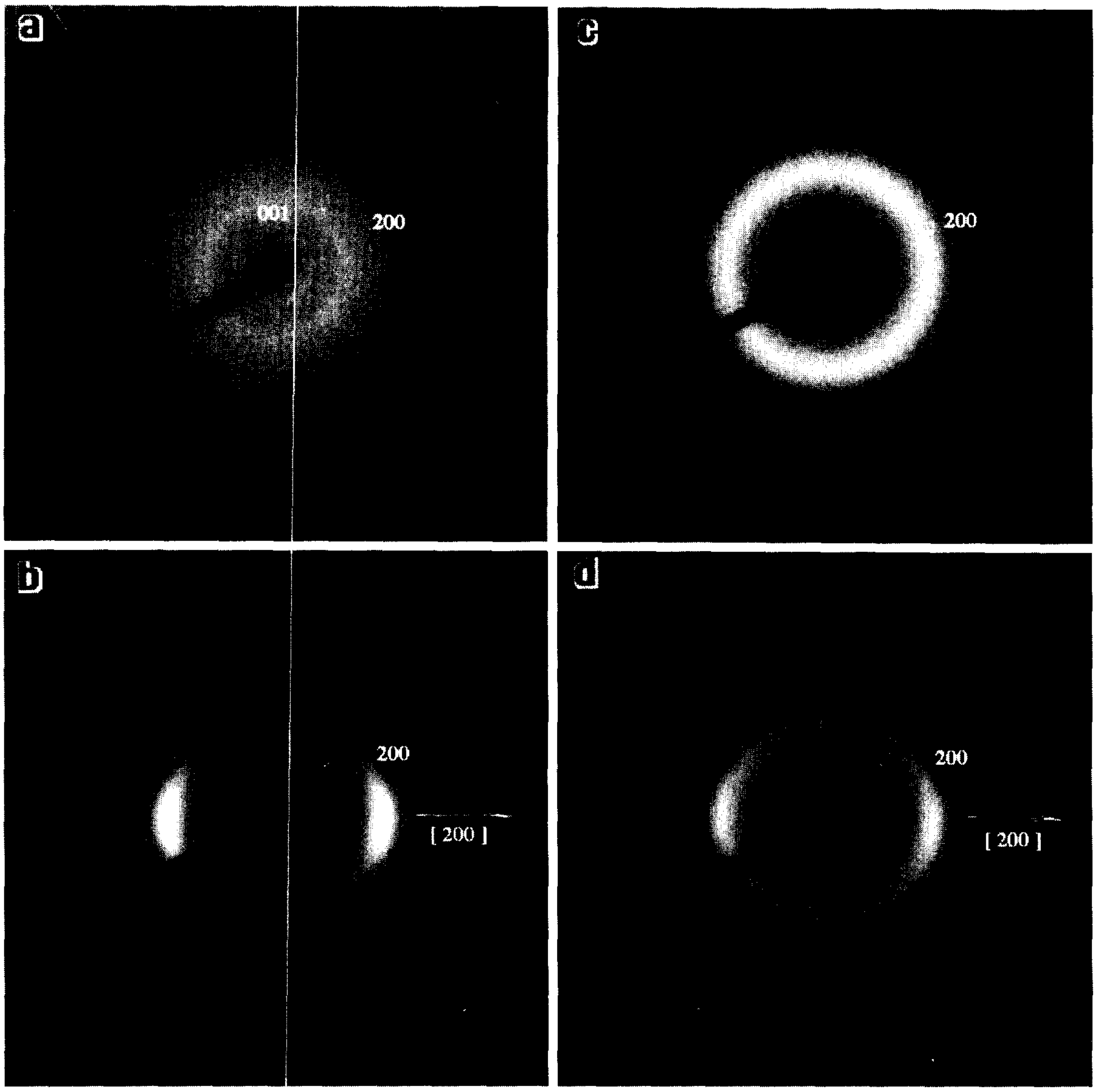

Figure 4 Diffraction patterns of unstretched films of MEH-PPV drop-cast from THF: a fresh sample under (a) perpendicular and (b) parallel settings, and a sample after degradation in the ambient atmosphere for 1 month under (c) perpendicular and (d) parallel settings

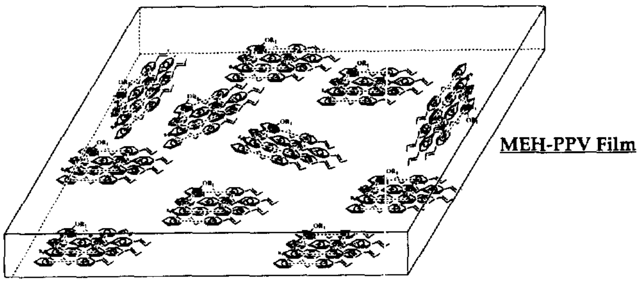

Figure 5 Schematic illustration of in-plane alignment of the crystalline domains in MEH-PPV film. The domains are drawn as ordered molecular chains. The benzene ring planes and the chain axes of the domains are lying in the plane of the MEH-PPV film but randomly oriented from one domain to another. The amorphous area is omitted for clarity

determines the anisotropy in the index of refraction. The latter plays a crucial role in the use of such films as planar waveguides, an aspect known to be critically important to the gain narrowing through amplified spontaneous emission.

We have followed the evolution of the microstructure of the films over time (samples were stored in air in the dark for a month). During this period we observed a re-orientation of the crystalline domains within the films, while the crystal structure did not appear to change. *Figure 4a* and *Figure 4b* are the diffraction patterns of a fresh MEH-PPV film cast from THF, while *Figure 4c* and *Figure 4d* are the patterns from the same batch of sample, after storage in the dark and in air for a month, for perpendicular and parallel settings respectively. Direct comparison of *Figure 4a* with *Figure 4c*, and *Figure 4b* with *Figure 4d* shows that the 200 reflection in *Figure 4a* (outside edge of the broad halo) is not evident, while it is very strong in *Figure 4c*. The arc in *Figure 4b* is prominent, but in *Figure 4d* it is almost completely blurred to a ring. These observations indicate that over a period of about 1 month, the films became nearly isotropic with chains almost equally oriented parallel to and perpendicular to the plane of the film.

Figure 7 shows the intensity profiles of the diffraction patterns for MEH-PPV/THF films in three different stages of aging: a fresh sample (corresponding to highest peak of the 200 reflection-continuous line in *Figure 7*), a sample after storage for 1 month in the ambient atmosphere (the lowest peak—broken line), and a sample kept in a

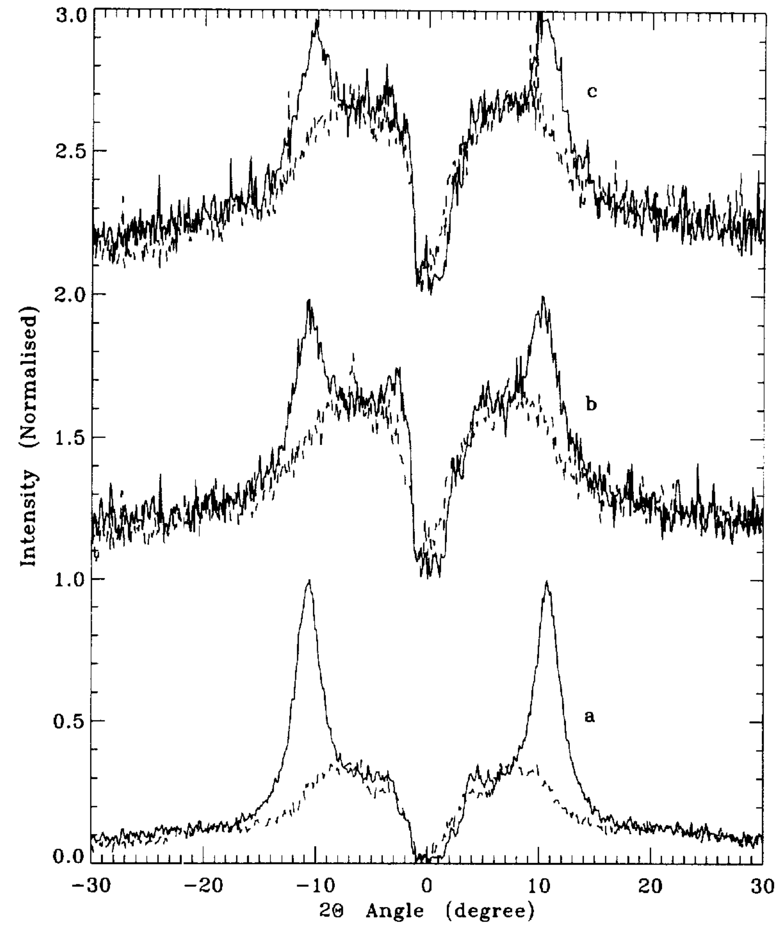

Figure 6 Intensity profiles, normalized to the maximum peak, of the diffraction patterns of unstretched MEH-PPV films drop-cast from (a) THF, (b) *p*-xylene, and (c) CB. Continuous line: profile along the [200] direction; broken line: perpendicular to the [200] direction

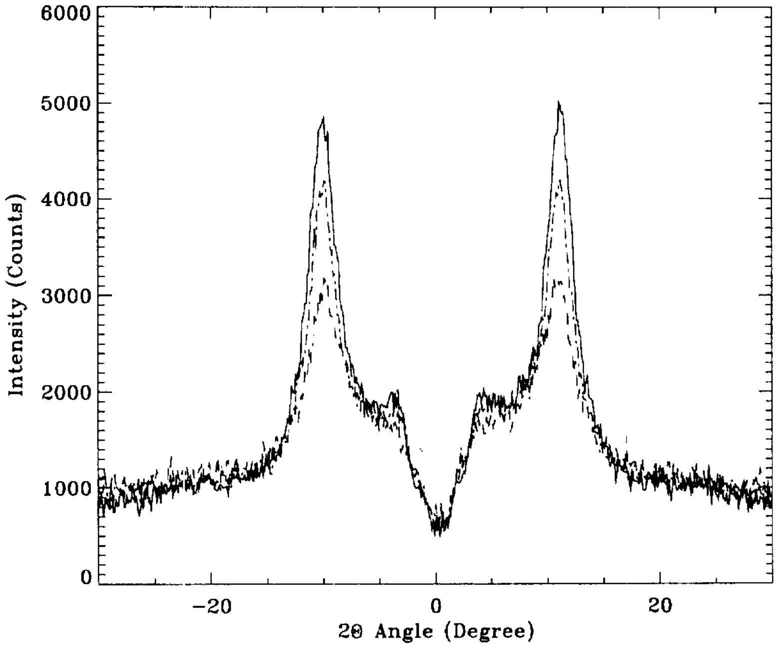

Figure 7 Intensity profile along the [200] direction for unstretched MEH-PPV films at different stages of degradation; continuous line (largest peak): fresh sample; broken line (smallest peak): sample after storage in the ambient atmosphere for 1 month; dashed line (medium peak): sample after storage in vacuum for 1 month

vacuum of 10^{-2} Torr for 1 month (the peak in the middle—dashed line). It is clear that the degradation rate, as measured by the anisotropic distribution of ordered benzene ring planes or the crystalline domains, is related to exposure to oxygen. At this point, one can only speculate on the mechanism by which this interesting chain re-orientation takes place.

CONCLUSION

In summary, the microstructure of MEH-PPV films has been investigated by X-ray diffraction and correlated with photopumped gain narrowing experiments. For MEH-PPV, independent of the solvent from which the films are drop-cast, the benzene ring planes are predominantly parallel to the plane. However, films drop-cast from THF, the best solvent for forming films with low threshold for gain narrowing and with narrow linewidth above threshold, show the highest degree of the anisotropy of in-plane chain orientation, the highest crystallinity, and the largest structural coherence lengths. Therefore, the choice of the solvent from which the films are prepared can be used to control the microstructure of the films, and hence improve the utility of the polymer as a material for use in solid-state lasers.

ACKNOWLEDGEMENTS

We thank Professor S. Tolbert and Professor B. J. Schwartz (UCLA) for valuable assistance and discussions. M. A. Díaz-García is supported by the Government of Spain. This research was supported by the National Science Foundation through the Materials Science and Engineering Center at UCSB (NSF-DMR 96-32716).

REFERENCES

1. Hide, F., Schwartz, B. J., Díaz-García, M. A. and Heeger, A. J., *Chem. Phys. Lett.*, 1996, **256**, 424.
2. Hide, F., Díaz-García, M. A., Schwartz, B. J., Andersson, M. R., Pei, Q. and Heeger, A. J., *Science*, 1996, **273**, 1833.
3. Hide, F., Díaz-García, M. A., Schwartz, B. J. and Heeger, A. J., *Accts. Chem. Res.*, in press.
4. Tessler, N., Denton, G. J. and Friend, R. H., *Nature*, 1996, **382**, 695.
5. Díaz-García, M. A., Hide, F., Schwartz, B. J., McGehee, M. D., Andersson, M. R. and Heeger, A. J., *Appl. Phys. Lett.*, 1997, **70**, 3191.
6. McGehee, M., Hide, F., Díaz-García, M. A., Schwartz, B. J., Moses, D. and Heeger, A. J., *Bull. Am. Phys. Soc.*, 1997, **42**, 645.
7. Brouwer, H.-J., Krasnikov, V. V., Hilberer, A., Wildeman, J. and Hadziioannou, G., *Appl. Phys. Lett.*, 1995, **66**, 3404.
8. Holzer, W., Penzkofer, A., Gong, S.-H., Bleyer, A. and Bradley, D. D. C., *Adv. Mater.*, 1996, **8**, 974.
9. Brouwer, H.-J., Krasnikov, V. V., Hilberer, A. and Hadziioannou, G., *Adv. Mater.*, 1996, **8**, 935.
10. Frolov, S. V., Ozaki, M., Gellerman, W., Vardeny, Z. V. and Yoshino, K., *Jpn. J. Appl. Phys.*, 1996, **35**, L1371.
11. Guinier, A., *X-ray Diffraction in Crystals, Imperfect Crystals, and Amorphous Bodies* (P. Lorrain and D. S.-M. Lorrain, Trans.), W. H. Freeman, San Francisco, 1963.
12. Vainshtein, B. K., *Diffraction of X-Rays by Chain Molecules*, Elsevier, Amsterdam, 1966.
13. Murthy, N. S. and Minor, H., *Polymer*, 1990, **31**, 996.